EXPERIMENTAL OVERVIEW OF ELECTROMAGNETIC PROBES IN ULTRA-RELATIVISTIC NUCLEUS–NUCLEUS COLLISIONS*

Klaus Reygers

Physikalisches Institut, Heidelberg University, Germany

Received 1 August 2022, accepted 16 September 2022, published online 14 December 2022

Electromagnetic probes are not affected by hadronization and provide direct information about the space-time evolution of high-energy nucleus–nucleus collisions. In particular, the measurement of thermal radiation from the quark–gluon plasma and the extraction of an effective medium temperature belong to the key objectives in heavy-ion physics. We provide a brief tour of current results and an outlook on future measurements.

DOI:10.5506/APhysPolBSupp.16.1-A19

1. Introduction

Once electroweak probes (γ, γ^*, W, Z) are produced in a high-energy nucleus–nucleus collision, they leave the surrounding medium with virtually no further interactions. The direct information these probes provide about the medium is therefore different from the information from light- and heavy-quark observables which are affected by hadronization. Electroweak bosons provide information about the entire evolution of a nucleus–nucleus collision. Parton distribution functions in nuclei are probed by measuring γ, γ^*, W, Z produced in the initial hard-scattering processes. Moreover, parton energy loss in the medium can be studied by measuring quark jets recoiling from a photon or a Z boson. Real and virtual photons produced in the preequilibrium phase, the quark–gluon plasma (QGP), and the hadron gas provide information about the space-time evolution and the temperature of the medium. In addition, the broadening of the ρ resonance in nucleus–nucleus collisions accessible via the decay $\rho \to e^+e^-$ is sensitive to the restoration of chiral symmetry [1]. This paper focuses on thermal radiation from the hot medium created in the high-energy nucleus–nucleus collision.

* Presented at the 29$^{\rm th}$ International Conference on Ultrarelativistic Nucleus–Nucleus Collisions: Quark Matter 2022, Kraków, Poland, 4–10 April, 2022.

Thermal photons from the QGP are expected to be a significant component of the direct-photon yield in the transverse momentum range $1 \lesssim p_{\mathrm{T}} \lesssim 3$ GeV/c [2, 3]. The inverse slope parameter T_{eff} is sensitive to the effective medium temperature averaged over the space-time evolution of the collision. Due to the rapid radial expansion of the medium, the measured photon spectrum is blueshifted and the inverse slope parameter is expected to be larger than the temperature of the emitting medium. Therefore, an inverse slope parameter above the critical temperature $T_{\mathrm{pc}} \approx 156$ MeV cannot be directly interpreted as evidence for the formation of a QGP. With increasing p_{T}, the measured direct-photon yield becomes more sensitive to earlier and hotter stages of collisions [4]. Photons from the preequilibrium stage could become important for $p_{\mathrm{T}} \gtrsim 2$–3 GeV/c [5].

Dileptons (virtual photons) probe different aspects of heavy-ion collisions depending on the considered mass range. Dileptons with invariant masses around and below the ρ-meson mass are particularly sensitive to modifications of the ρ meson due to the surrounding medium. These modifications are experimentally accessible as the ρ decays in the medium due to its short lifetime of only 1.3 fm/c. In particular, the presence of baryons in the medium is expected to give rise to ρ melting, *i.e.*, to a strong increase in its width. The ρ melting is connected to the restoration of chiral symmetry in a hot and dense medium. The intermediate-mass region (IMR, $1 \lesssim m_{ee} \lesssim 3$ GeV/c^2) is sensitive to thermal radiation from the QGP. An effective medium temperature not affected by blueshift can be obtained by fitting the dielectron yield in this range with $\mathrm{d}N/m_{ee} \propto (m_{ee}T)^{3/2} \exp(-m_{ee}/T)$. With increasing mass, the contribution from dielectrons from the preequilibrium stage becomes more relevant which needs to be considered in the extraction of a temperature. To date, the only measurement of a medium temperature in the mass range above 1 GeV/c^2 was made by the NA60 experiment at the CERN SPS in In–In collisions. A fit in the range $1.2 \lesssim m_{ee} \lesssim 2.0$ GeV/c^2 gave an effective temperature of $T = 205 \pm 12$ MeV [6].

2. Low-p_{T} direct photons

Direct photon measurements are expected to eventually play a key role in our understanding of the evolution of the QGP in nucleus–nucleus collisions. However, it is currently a challenge for models to simultaneously describe the direct-photons yield and the azimuthal anisotropy (v_2) of direct photons. This is known as the direct-photon puzzle [5, 7]. The puzzle became apparent at the Quark Matter 2011 conference with the observation by the PHENIX Collaboration that the v_2 of direct photons was similar to the v_2 of pions, whereas hydrodynamic models predicted a much smaller direct-photon v_2.

In addition, hydrodynamic models underestimated the direct photon yield at low p_{T} by about a factor of 2–3 [7]. The radial flow velocity profiles created in the hydrodynamic evolution of the medium need time to build up. The large direct-photon v_2, therefore, could mean that contrary to the general expectation, direct photons in the range of $1 \lesssim p_{\mathrm{T}} \lesssim 3$ GeV/c are predominantly produced at the later stages of the medium evolution, perhaps during the transition from the QGP to a gas of hadrons. This would make direct photons a less useful probe of the early hot QGP phase. The direct-photon puzzle currently is a puzzle which concerns the PHENIX spectra and v_2 measurements. At the LHC, the ALICE direct-photon spectra and v_2 measurements show similar trends as the PHENIX data, however, the uncertainties are unfortunately too large to claim a significant difference between data and theory.

At this conference, PHENIX presented the final direct-photon spectra in Au–Au collisions at $\sqrt{s_{NN}} = 200\,\mathrm{GeV}$ from the high-statistics 2014 data set [8]. A significant excess above the direct-photon spectrum in *pp* collisions at $\sqrt{s} = 200\,\mathrm{GeV}$ scaled by the number of nucleon–nucleon collisions (N_{coll}) is found. The difference between direct-photon spectra in Au–Au collisions and the scaled *pp* spectrum, denoted by PHENIX as "nonprompt" direct-photon spectrum, is shown in Fig. 1. PHENIX extracted the inverse slope parameter T_{eff} in two fit ranges for various centralities (see Fig. 1, right panel). The inverse slope parameter is independent of the centrality but increases with increasing p_{T}, in line with a larger early-time contribution at higher p_{T}.

To examine at which stage of a nucleus–nucleus collision direct photons are predominantly produced, it is instructive to study the dependence of the direct-photon yield on the centrality and center-of-mass energy. PHENIX found a universal scaling according to which the direct-photon yield integrated above $p_{\mathrm{T}} = 1\,\mathrm{GeV}/c$ is a function of the charged-particle multiplicity alone (for different centralities, center-of-mass energies, and collision systems) and is given by $\mathrm{d}N_\gamma^{\mathrm{dir}}/\mathrm{d}y \propto (\mathrm{d}N_{\mathrm{ch}}/\mathrm{d}\eta|_{\eta\approx 0})^\alpha$, see Fig. 2. A fit to the 2014 data gives $\alpha = 1.11 \pm 0.02\,(\mathrm{stat.})^{+0.09}_{-0.08}\,(\mathrm{syst.})$. Interestingly, this value is smaller than the power $\alpha \approx 1.6$ expected for thermal photons in [4]. Photons from different stages of a collision are actually expected to exhibit a different scaling behavior. In [4], it is predicted that the hadron gas, the QGP, and hard scattering contributions scale as $\alpha_{\mathrm{HG}} \approx 1.23$, $\alpha_{\mathrm{QGP}} \approx 1.83$, and $\alpha_{\mathrm{pQCD}} \approx 1.25$, respectively. Different stages contribute differently to different p_{T} intervals and one might expect a strong p_{T} dependence of α. PHENIX, however, finds that $\alpha(p_{\mathrm{T}})$ is consistent with being independent of p_{T}.

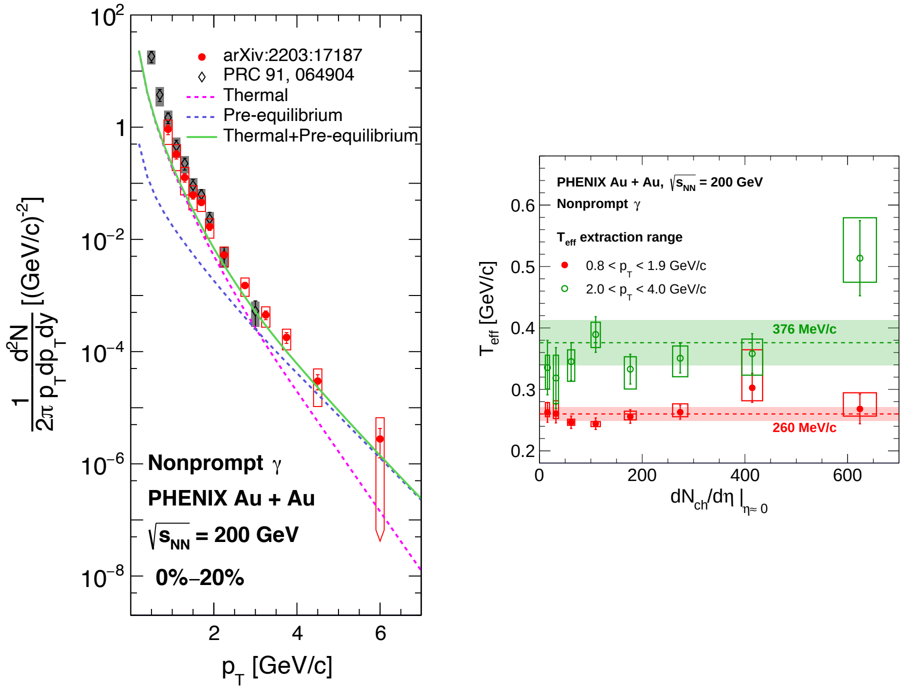

Fig. 1. Left panel: Nonprompt ("Au–Au $-N_{\mathrm{coll}} \times pp$") direct-photon spectrum in central Au–Au collisions at $\sqrt{s_{NN}} = 200$ GeV [8]. The new data from the high-statistics 2014 Au+Au run are shown as closed circles. Right panel: Inverse slope parameters T_{eff} in Au–Au collisions at $\sqrt{s_{NN}} = 200$ GeV for different centralities characterized by the charged-particle multiplicity density $\mathrm{d}N_{\mathrm{ch}}/\mathrm{d}\eta|_{\eta\approx 0}$.

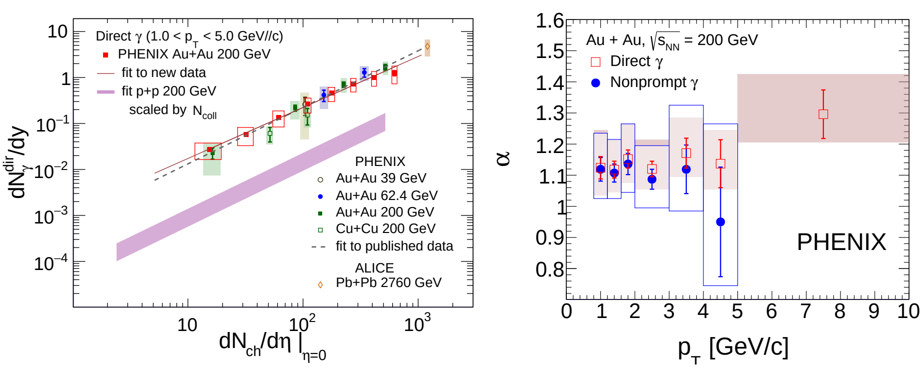

Fig. 2. Left panel: Direct photon yield $\mathrm{d}N_\gamma^{\mathrm{dir}}/\mathrm{d}y$ in the range of $1 < p_{\mathrm{T}} < 5\,\mathrm{GeV}/c$ for collisions with different charged-particle multiplicity densities $\mathrm{d}N_{\mathrm{ch}}/\mathrm{d}\eta|_{\eta\approx 0}$. Right panel: Scaling power α describing the charged-particle multiplicity dependence of the direct-photon yield in different p_{T} intervals according to $\mathrm{d}N_\gamma^{\mathrm{dir}}/\mathrm{d}y \propto (\mathrm{d}N_{\mathrm{ch}}/\mathrm{d}\eta|_{\eta\approx 0})^\alpha$.

ALICE showed new preliminary direct-photon spectra in Pb–Pb collisions at $\sqrt{s_{NN}} = 5.02$ TeV [9]. The results of two independent methods, the photon conversion method and the virtual photons method, were found to be in agreement, see Fig. 3. Photons from the initial hard parton–parton scatterings as obtained from a scaled next-to-leading-order perturbative QCD (pQCD) calculation are sufficient to explain the data. A calculation with additional contributions from thermal and preequilibrium photons also agrees with the data. To establish a signal of thermal photons in nucleus–nucleus collisions at the LHC thus requires a further reduction of the experimental uncertainties.

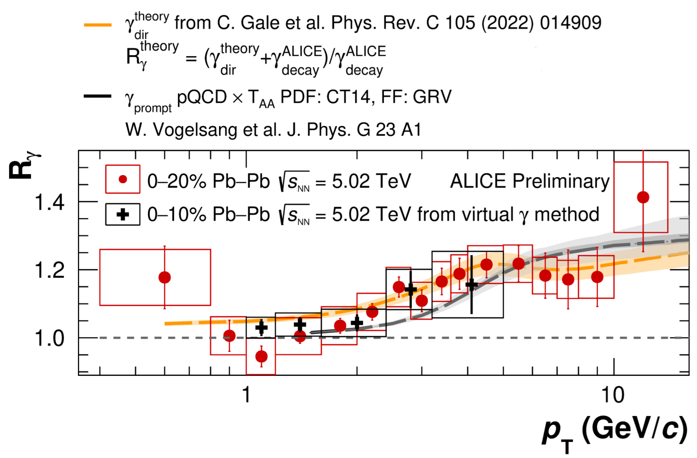

Fig. 3. (Color online) Direct-photon excess ratio $R_\gamma = \gamma_{\rm total}/\gamma_{\rm decay} \equiv 1 + \gamma_{\rm direct}/\gamma_{\rm decay}$ in the central Pb–Pb collisions at $\sqrt{s_{NN}} = 5.02$ TeV. A scaled pQCD calculation (gray dashed line) and a model with additional photon production sources including thermal radiation from the QGP (light gray/orange dashed line) are compared to the data.

With the calculation of [5] and the new direct-photon spectra presented at this conference, the differences between data and theory in terms of the yields do not appear very significant anymore, see Fig. 4. At low $p_{\rm T} \lesssim 3$ GeV/c, where thermal and preequilibrium photons are expected, one finds good agreement of the model calculation with the LHC measurements. At RHIC, the model predictions agree with the STAR data [10] at low $p_{\rm T}$. The calculation is systematically below the PHENIX data, however, within the experimental systematic uncertainties, there is no significant deviation. While the puzzle appears almost resolved concerning the yields, it remains a challenge to explain the large azimuthal anisotropy (v_2) measured by PHENIX.

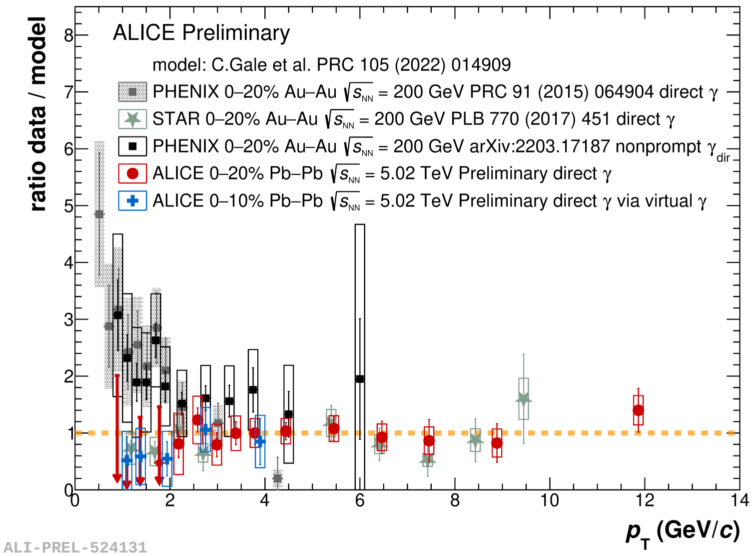

Fig. 4. Comparison of direct-photon transverse momentum spectra measured at RHIC and the LHC to a model which includes thermal and preequilibrium photons in addition to pQCD photons.

3. Dileptons

ALICE presented a preliminary dielectron mass spectrum in central Pb–Pb collisions at $\sqrt{s_{NN}} = 5.02$ TeV at this conference, see Fig. 5 [11]. To establish a signal of thermal radiation in the low-mass region (LMR, $m_{ee} \lesssim 1\,\mathrm{GeV}/c^2$) and in the intermediate-mass region (IMR, $1 \lesssim m_{ee} \lesssim 3\,\mathrm{GeV}/c^2$) at LHC energies, a detailed understanding of e^+e^- pairs resulting from correlated semileptonic decays of open charm and beauty hadrons is crucial ($c\bar{c} \to e^+e^-$, $b\bar{b} \to e^+e^-$). In Fig. 5, two versions of the cocktail, with and without nuclear modification of the $c\bar{c} \to e^+e^-$ and $b\bar{b} \to e^+e^-$ contribution, are compared to the data. In both cases, no clear enhancement above the cocktail is observed. However, predictions that include thermal QGP radiation and a medium-modified ρ also appear to be consistent with the data. Separation of the prompt thermal signal from the nonprompt background of semileptonic decays based on the distance of the closest approach of the electron and positron tracks to the primary interaction point will play a crucial role in the extraction of a thermal signal.

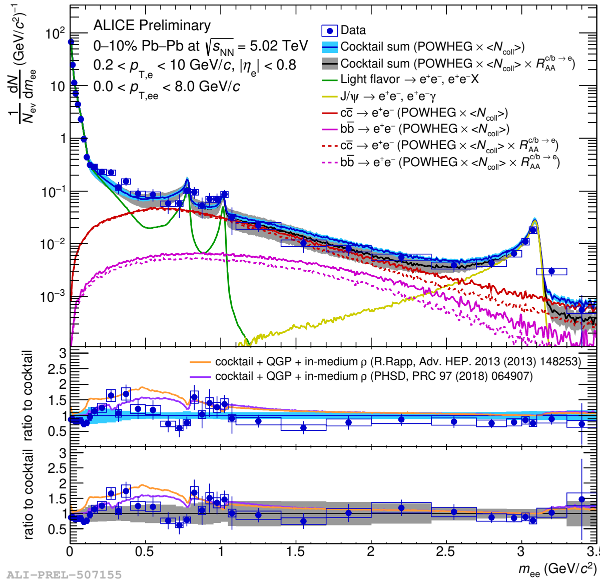

Fig. 5. Dielectron invariant mass distribution in central Pb–Pb collisions at $\sqrt{s_{NN}} = 5.02$ TeV after subtraction of uncorrelated background. The data are compared to the expected yield ("cocktail") from the decay of hadrons (light-flavor hadrons and J/ψ) and from e^+e^- pairs resulting from correlated semileptonic open-charm and open-beauty hadron decays. The two lower panels show the comparison of two versions of the cocktail, with and without nuclear modifications of the $c\bar{c} \to e^+e^-$ and $b\bar{b} \to e^+e^-$ contribution.

4. Future measurements

One of the main current goals in the study of electromagnetic probes is to obtain a global picture of high-energy nucleus–nucleus collisions in which both electromagnetic observables as well as light- and heavy-quark observables can be naturally explained. This entails the determination of a unique signal of thermal radiation as well as the extraction of an effective medium temperature. An effective medium temperature above the critical temperature $T_{\rm pc} \approx 156\,\text{MeV}$ would provide additional evidence for the formation of a QGP. To improve our understanding of the QCD phase diagram, future measurements of electromagnetic probes at vanish and high baryo-chemical potential μ_B play a crucial role, see Table 1. These include, *e.g.*, the study of the caloric curve ($T_{\rm eff}$ as a fct. of $\sqrt{s_{NN}}$) to find evidence for a first-order phase transition at high μ_B. In addition, real and virtual photons at very low $p_{\rm T}$ (and masses) could provide information about the electrical conductivity of the QGP. Moreover, the long-standing puzzle of the measured excess of ultra-soft photons above predictions based on Low's theorem [12] should finally be resolved.

Table 1. Possible future measurements of electromagnetic observables at high and vanishing baryochemical potential $\mu_{\rm B}$ along with the corresponding experiments [13, 14].

	High $\mu_{\rm B}$	Vanishing $\mu_{\rm B}$
Thermal radiation (γ, γ^* spectra)	STAR, NA60+, CBM, NICA	PHENIX, STAR, ALICE 2, ALICE 3
Caloric curve ($T_{\rm eff}$ in IMR *vs.* $\sqrt{s_{NN}}$)	STAR, NA60+, CBM, NICA	
Mechanism of chiral symmetry resoration, ρ–a_1 mixing	CBM, NA60+	STAR, ALICE 3
Dilepton + direct photon v_n	CBM, HADES, NA60+	STAR, (ALICE 2), ALICE 3
Time dep. of $T_{\rm eff}$, preequilibrium contrib.		ALICE 3
Ultra-soft photons (test of Low's theorem)		ALICE 3
Electrical conductivity	HADES	STAR, ALICE 3

REFERENCES

[1] R. Rapp, *AIP Conf. Proc.* **1322**, 55 (2010).
[2] G. David, *Rep. Prog. Phys.* **83**, 046301 (2020).
[3] A. Monnai, *Int. J. Mod. Phys. A* **37**, 2230006 (2022).
[4] C. Shen, U.W. Heinz, J.-F. Paquet, C. Gale, *Phys. Rev. C* **89**, 044910 (2014).
[5] C. Gale, J.-F. Paquet, B. Schenke, C. Shen, *Phys. Rev. C* **105**, 014909 (2022).
[6] H.J. Specht, *AIP Conf. Proc.* **1322**, 1 (2010).
[7] J.-F. Paquet *et al.*, *Phys. Rev. C* **93**, 044906 (2016).
[8] PHENIX Collaboration, `arXiv:2203.17187 [nucl-ex]`.
[9] M.C. Danisch, *Acta Phys. Pol. B Proc. Suppl.* **16**, 1-A122 (2023), this issue.
[10] STAR Collaboration, *Phys. Lett. B* **770**, 451 (2017).
[11] J. Jung, *Acta Phys. Pol. B Proc. Suppl.* **16**, 1-A124 (2023), this issue.
[12] F.E. Low, *Phys. Rev.* **110**, 974 (1958).
[13] NA60+ Collaboration, Tech. Rep. CERN-SPSC-2019-017; SPSC-EOI-019, CERN, 2019.
[14] ALICE Collaboration, Tech. Rep. CERN-LHCC-2022-009; LHCC-I-038, CERN, 2022.